J. Fluid Mech. (1977), *vol.* 81, *part* 1, *pp.* 187–207
Printed in Great Britain

Influence of helicity on the evolution of isotropic turbulence at high Reynolds number

By J. C. ANDRÉ

Direction de la Météorologie, EERM/GMD, Paris, France

AND M. LESIEUR

Centre National de la Recherche Scientifique, Observatoire de Nice, France†

(Received 2 April 1976 and in revised form 28 December 1976)

Three-dimensional homogeneous isotropic turbulence at very high Reynolds number R is studied using a variant of the Markovian eddy-damped quasi-normal theory. In the case without helicity, numerical calculations indicate the development of a $k^{-\frac{5}{3}}$ inertial range in the energy spectrum and an onset of significant energy dissipation at a time t_* which appears to be independent of the viscosity ν as $\nu \to 0$; analytical arguments having a bearing on this behaviour, described as an 'energy catastrophe', are also discussed. The skewness factor (for $t > t_*$), which increases with R, tends to 0·495 when $R \to \infty$. When helicity is present, the existence of simultaneous energy and helicity cascades is demonstrated numerically. It is also shown that the helicity cascade inhibits the energy transfer towards large wavenumbers, in agreement with preliminary low Reynolds number results of Herring and with the conclusion of Kraichnan (1973) based on analysis of the interaction between two helicity waves. This inhibition implies a delay of the onset of energy dissipation at zero viscosity. It is shown that, whatever the relative rate of helicity and energy injection, a regime is attained at large wavenumbers k where the relative helicity tends to zero (with increasing k) and helicity is carried along locally and linearly by the energy cascade like a passive scalar. In practice, the linear regime is attained when the relative helicity is less than about 10 %. The Kolmogorov constants of energy and helicity in the inertial range are determined. The impossibility of pure helicity cascades of a type conjectured by Brissaud *et al.* (1973*a*) is demonstrated. Finally it is shown that, because of dissipation and non-positive-definiteness of the helicity spectrum, non-zero total helicity may appear in the decay of unforced turbulence with zero total initial helicity, if the helicity spectrum is not initially identically zero.

1. Introduction

Helicity $\langle \mathbf{u} . \operatorname{curl} \mathbf{u} \rangle$, which is an inviscid invariant of three-dimensional homogeneous turbulence (Betchov 1961; Moffatt 1969), is known to play an important part in the generation of magnetic fields (Steenbeck, Krause & Rädler 1966; Moffatt 1970*a*, *b*; Frisch *et al.* 1975; Pouquet Frisch & Léorat 1976). In this paper we are going to consider

† Present address: Institut de Mécanique de Grenoble, 38041 Grenoble-Cédex, France.

the influence of helicity on the dynamics of flows in the absence of magnetic field. We shall introduce energy and helicity spectra $E(k,t)$ and $H(k,t)$ such that

$$\langle \mathbf{u}^2(t) \rangle = \int_0^\infty E(k,t)\,dk, \tag{1.1}$$

$$\langle \mathbf{u}(t) . \operatorname{curl} \mathbf{u}(t) \rangle = \int_0^\infty H(k,t)\,dk. \tag{1.2}$$

It may be shown that
$$|H(k,t)| \leqslant kE(k,t). \tag{1.3}$$

This result follows from the definition of vorticity in the case of a discrete velocity spectrum (flow within a box of size L with periodic boundary conditions) and can be extended to homogeneous turbulence by letting L become infinite.

From the conservation of helicity, Brissaud *et al.* (1973*a*) conjectured on a phenomenological basis two types of cascade: (i) simultaneous energy and helicity cascades where the helicity is carried linearly along the energy cascade; (ii) a pure helicity cascade towards large wavenumbers with a $k^{-\frac{7}{3}}$ energy spectrum and no energy transfer. Such a helicity cascade would then imply an inverse $k^{-\frac{5}{3}}$ energy cascade towards small wavenumbers with no helicity transfer. The existence of this type (ii) cascade is, however, in some doubt; indeed Kraichnan (1973) observed that, starting from initial conditions with maximal helicity [expressed by equality in (1.3)], it was impossible to have a direct helicity transfer without any energy transfer since this would violate (1.3). In § 4 we shall show that, within the framework of the particular scheme adopted below, the second type of cascade is in fact impossible.

In this paper, we study helical turbulence using a variant of the Markovian eddy-damped quasi-normal (EDQN) theories introduced by Orszag (1970) and Leith (1971). These theories are characterized by a relaxation time $\theta_{kpq}(t)$ for triple correlations (Kraichnan 1971*a*; Sulem, Lesieur & Frisch 1975), which is here taken to be

$$\theta_{kpq}(t) = t/[1 + (\mu_k + \mu_p + \mu_q)\,t], \tag{1.4}$$

with
$$\mu_k = \nu k^2 + \lambda \left\{ \int_0^k p^2 E(p)\,dp \right\}^{\frac{1}{2}}, \tag{1.5}$$

where λ is an adjustable constant which may be chosen so as to recover the proper value of the Kolmogorov constant. In fact (J. Herring, private communication) the EDQN theory characterized by (1.5), and previously used by Pouquet *et al.* (1975) to study the temporal evolution of two-dimensional turbulence, can be considered as a simplification of the test-field model (Kraichnan 1971*a*). In § 4 we derive the relation between the Kolmogorov constant C_E and the parameter λ, and find that

$$\lambda = 0{\cdot}109 C_E^{\frac{3}{2}}, \tag{1.6}$$

so that we must take $\lambda = 0{\cdot}255$ to recover for C_E the value 1·76† estimated by Kraichnan (1971*b*).

† In Kraichnan's notation the energy spectrum was defined by

$$\tfrac{1}{2}\langle \mathbf{u}^2(t) \rangle = \int_0^\infty E(k,t)\,dk,$$

so that we must multiply our Kolmogorov constant by $2^{-\frac{1}{3}}$ to find Kraichnan's value 1·4.

2. Evolution of non-helical turbulence

The problem of the regularity of solutions of the three-dimensional Euler equations (i.e. the inviscid Navier–Stokes equations) has received much attention in the last few years (Ebin & Marsden 1970; Kato 1972). There are at present various conjectures concerning a possible loss of regularity of the solutions of the Euler equations after a finite time depending upon initial conditions (Orszag 1976; Brissaud *et al.* 1973*b*; Lesieur & Sulem 1976). In Brissaud *et al.* (1973*b*) this conjecture is based on the study of the Markovian random coupling model (the MRC model; see Frisch, Lesieur & Brissaud 1974) applied to the Burgers equation, where it is shown that

(*a*) when $\nu = 0$, energy is conserved up to a finite time t_* at which the enstrophy (which is in this case defined as the mean value of the square of the velocity gradient) becomes infinite;

(*b*) when $\nu \to 0$, energy is conserved for $t < t_*$ and is dissipated at a finite rate after t_* (Penel 1975).

The behaviour described by the two properties (*a*) and (*b*) will be called an 'energy catastrophe'.

Let $D(t)$ be the enstrophy in the inviscid case and $D_\nu(t)$ the enstrophy in the viscous case for the same initial conditions. If one assumes that

$$\lim_{\nu \to 0} D_\nu(t) = D(t), \tag{2.1}$$

then (*b*) implies (*a*), since the energy dissipation rate $2\nu D_\nu(t)$ cannot be finite in the limit $\nu \to 0$ unless $D_\nu(t)$ becomes infinite. On the other hand (*a*) does not necessarily imply (*b*).† Furthermore it must be noticed that the existence of a $k^{-\frac{5}{3}}$ energy spectrum extending to infinite wavenumber when $\nu \to 0$ implies an infinite enstrophy and also a constant energy transfer rate across any arbitrarily large wavenumber.

In this section we shall investigate the possibility of an energy catastrophe using the EDQN theory applied to three-dimensional homogeneous and isotropic turbulence without helicity. In the following sections we shall study how these results are modified by helicity.

The EDQN equation for the energy spectrum $E(k, t)$ is

$$\left(\frac{\partial}{\partial t} + 2\nu k^2\right) E(k,t) = \frac{1}{2} \iint_{\Delta_k} \frac{k}{pq} \theta_{kpq}(t)\, b_3(k,p,q) \times \{k^2 E(p,t)\, E(q,t) - p^2 E(q,t)\, E(k,t)\}\, dp\, dq, \tag{2.2}$$

where $b_3(k,p,q) = (p/k)(xy + z^3)$ is the geometrical coefficient introduced by Kraichnan for three-dimensional turbulence (x, y and z being the cosines of the angles opposite to sides k, p and q in the interacting triad). This notation is the same as that in Frisch *et al.* (1974). The numerical methods used in this section and in the following ones are the same as those in Pouquet *et al.* (1975). The double integral in (2.2) is calculated in the same way as in Leith (1971). Wavenumbers are discretized logarithmically,

$$k_L = k_{\min} 2^{L/F}, \quad L = 0, \ldots, L_{\max}, \quad F = 4, \tag{2.3}$$

† In fact, if the EDQN spectral equation is analytically continued to non-integer dimension d, it is found numerically that enstrophy blows up at a finite time but energy is nevertheless conserved for $2 < d < d_c$, where $d_c \approx 2{\cdot}03$ (Frisch, Lesieur & Sulem 1976).

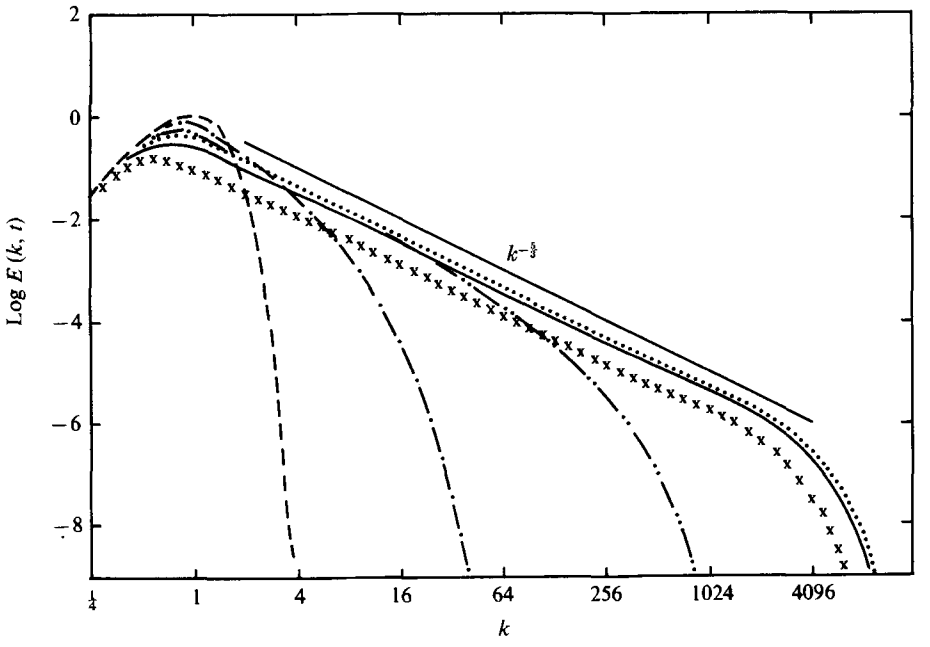

FIGURE 1. Temporal evolution of energy spectrum $E(k, t)$; no helicity, initial spectrum $E(k, 0) \sim k^4 \exp(-2k^2)$, Reynolds number $R = 524000$. – –, $t = 0$; –·–, $t = 3$; –···–, $t = 5$; ·····, $t = 6$; ——, $t = 8$; xxx, $t = 15$.

and the largest wavenumber $k_{\max}$ retained in the numerical calculation must be sufficiently large to include the dissipation range characterized by the Kolmogorov dissipation wavenumber k_D:

$$k_D \sim (\epsilon/\nu^3)^{\frac{1}{4}}, \tag{2.4}$$

where

$$\epsilon = \epsilon(t) = -\frac{d}{dt}\langle \mathbf{u}^2(t)\rangle = 2\nu \int_0^\infty k^2 E(k, t)\, dk \tag{2.5}$$

is the dissipation rate. If k_I is the wavenumber characteristic of energy-containing eddies, and assuming, for instance, an energy spectrum proportional to $\epsilon^{\frac{2}{3}} k^{-\frac{5}{3}}$ extending from k_I to k_D, it is easy to show that

$$k_D/k_I \sim R^{\frac{3}{4}}, \tag{2.6}$$

where the large-scale Reynolds number R is defined as

$$R = \langle \mathbf{u}^2(0)\rangle^{\frac{1}{2}}/\nu k_I. \tag{2.7}$$

In all the calculations to be reported we have taken $k_{\max}/k_I = 8R^{\frac{3}{4}}$, and checked that a further increase in $k_{\max}$ for a given Reynolds number left the results unchanged; moreover it can be seen that all the computed energy spectra (figures 1, 6 and 7) include a properly described dissipation range.

In figure 1 the time evolution of an initial energy spectrum

$$E(k, 0) = \frac{32}{3}\left(\frac{2}{\pi}\right)^{\frac{1}{2}} k^4 \exp(-2k^2) \tag{2.8}$$

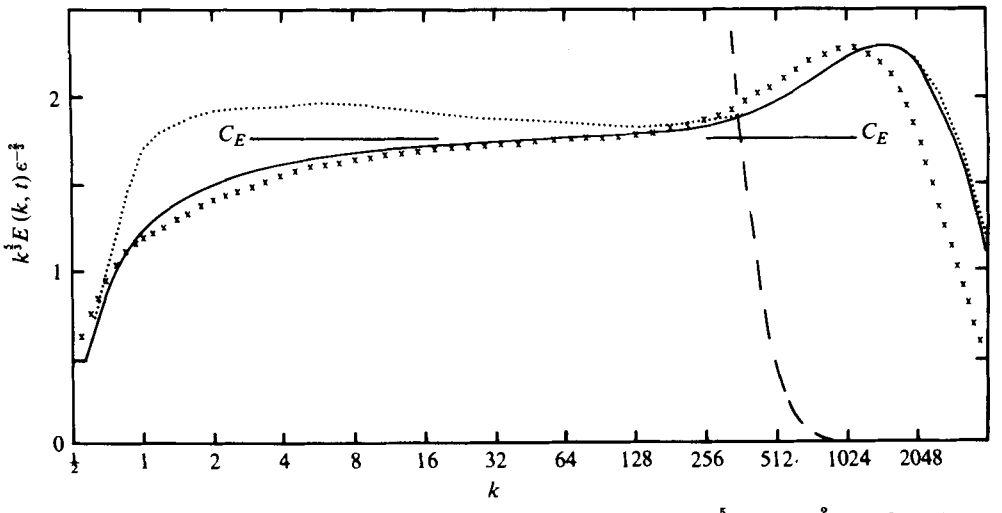

FIGURE 2. Variation of the energy compensated spectrum $k^{\frac{5}{3}}E(k,t)\,\epsilon^{-\frac{2}{3}}$ as a function of k; same conditions as in figure 1. – –, $t = 5$; ····, $t = 6$; ——, $t = 8$; xxx, $t = 15$.

is reported on a log–log plot. The units are k_I for k, $\langle \mathbf{u}^2(0)\rangle^{-\frac{1}{2}}k_I^{-1}$ for t and $\langle \mathbf{u}^2(0)\rangle/k_I$ for $E(k,t)$. The Reynolds number in this numerical experiment is 524 000. As can be seen a $k^{-\frac{5}{3}}$ Kolmogorov inertial range is established at $t = 6$ and extends over more than three decades. For larger times, the spectrum in the inertial range remains proportional to $\epsilon^{\frac{2}{3}}k^{-\frac{5}{3}}$. The temporal evolution will then be determined by $\epsilon(t)$ alone. In the numerical calculation one finds $\epsilon(6) = 0{\cdot}120$, $\epsilon(8) = 0{\cdot}103$ and $\epsilon(15) = 0{\cdot}028$. It follows that the curves for $t = 6$ and $t = 8$ are almost identical, while the extent of the inertial range at $t = 15$ has been reduced by a factor of about 1·4. In figure 2 we have plotted for various times the compensated spectrum $k^{\frac{5}{3}}\epsilon^{-\frac{2}{3}}E(k,t)$. (Log–log plots alone are inadequate because they underestimate deviations from power laws.) At $t = 5$, where the Kolmogorov inertial range has not yet been established and where the energy spectrum is always rapidly decreasing, the compensated spectrum is sharply peaked and only its right end is represented. It can be seen at $t = 8$ that the value of the compensated spectrum remains constant and equal to 1·76 to within 11 % from $k = 4$ to $k = 512$.

Figure 3 shows the energy transfer rate across a wavenumber K:

$$\pi(K,t) = \int_K^\infty T(k,t)\,dk, \tag{2.9}$$

where $T(k,t)$ represents the right-hand side of (2.2). For $t = 8$, $\pi(k,t)$ is equal to 0·085 to within 18 % from $k = 4$ to $k = 512$. In this experiment the energy dissipation rate ϵ is equal to 0·103.

To improve the results shown in figures 2 and 3, it would be necessary to increase the Reynolds number, but this would require a lot of computer time; it took 1200 s on a CDC 6600 machine to compute the evolution of the energy spectrum from $t = 0$ to $t = 15$. This kind of calculation in Fourier space cannot be performed in the inviscid case with conservative numerical schemes (i.e. those which conserve energy and helicity for the nonlinear terms) since it is well known that a finite number of modes leads then to a k^2 absolute equilibrium spectrum (Lee 1952). The influence of helicity on absolute

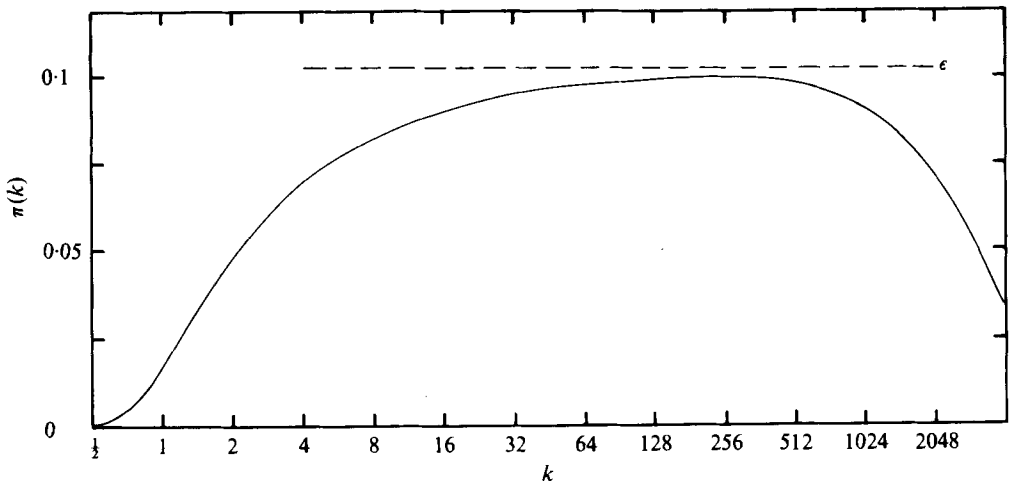

FIGURE 3. Variation of the energy transfer rate $\pi(k,t)$ as a function of k for $t = 8$; same conditions as in figure 1. – – –, energy dissipation rate ϵ.

equilibrium distributions has been studied by Kraichnan (1973) and Frisch *et al.* (1975). It would of course be interesting to integrate the inviscid form of (2.2) with a finite number of modes but this would require a parametrization of the interactions with the modes not represented. This is a particular case of the very difficult 'parametrization problem', which has been studied for the two-dimensional EDQN equation by Basdevant, Lesieur & Sadourny (1976).

The compensated spectra in figure 2 exhibit a bump at large wavenumbers. We have checked that this pathological effect does not disappear when the Reynolds number increases. It is probably due either to the particular closure or to the numerical procedure used to solve the master equation (2.2): the bump could be a consequence of the fact that the numerical method does not take into account the non-local interactions, except those corresponding to isosceles triads (Pouquet *et al.* 1975). These non-local interactions are not completely negligible in the inertial range (Kraichnan 1971*b*). This point is extensively discussed in § 4.

The formation of a $k^{-\frac{5}{3}}$ inertial range in the energy spectrum, which is established after $t \approx 5$ (as can be seen in figure 2), is related as follows to the occurrence of an 'energy catastrophe' at a finite time t_*.

(*a*) Following a calculation of Proudman & Reid (1954) in the case of the quasi-normal approximation, it can be shown (Lesieur 1973) in the simple case of the Markovian random coupling model ($\theta_{kpq}(t) = \theta_0$) that the enstrophy

$$D(t) = \int_0^\infty k^2 E(k,t)\, dk$$

satisfies
$$dD/dt = \tfrac{1}{3}\theta_0 D^2, \tag{2.10}$$

which implies that $D(t)$ blows up at $t_* = 3/(\theta_0 D(0))$. In the more complex case of the EDQN theory, we have not succeeded in demonstrating analytically the blow-up of enstrophy, but it can be shown (see appendix A) that $D(t)$ satisfies the inequality

$$dD/dt \leqslant 1{\cdot}07 D^{\frac{3}{2}}, \tag{2.11}$$

which implies that energy is conserved at least for times smaller than $1{\cdot}87 D^{-\frac{1}{2}}(0)$.

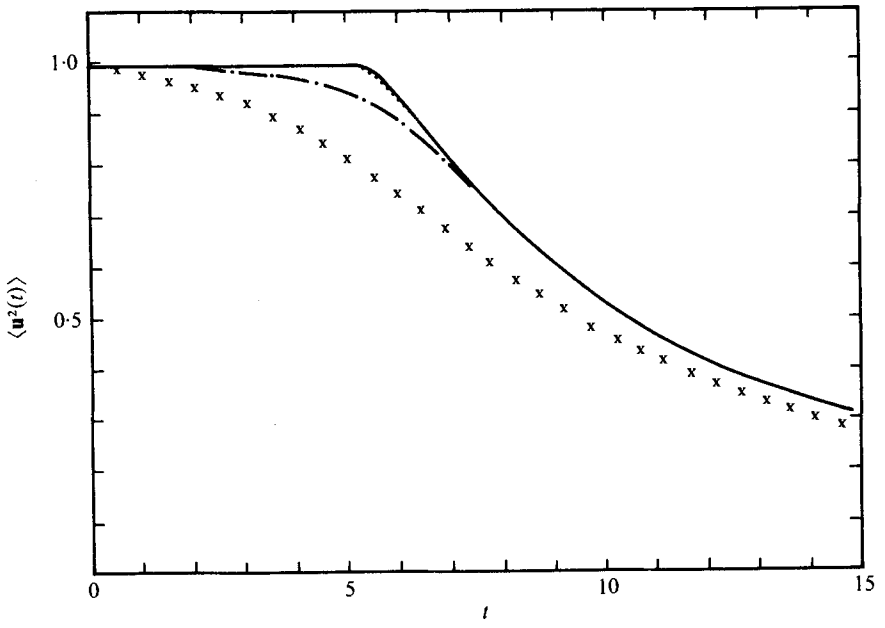

FIGURE 4. Temporal evolution of the total energy $\langle \mathbf{u}^2(t) \rangle$; same initial conditions as in figure 1. xxx, $R = 128$; –·–, $R = 813$; ·····, $R = 32800$; ——, $R = 524000$.

(*b*) It must be mentioned that the blow-up of enstrophy at a finite time can be obtained in the framework of the EDQN theory through a modification of $\theta_{kpq}(t)$. On changing $\theta_{kpq}(t)$ into $\theta_{lmn}(t)$, where $l = \sup(k, k')$, $m = \sup(p, p')$ and $n = \sup(q, q')$ with

$$k'^2 = p^2 + q^2 + 2pqx, \quad p'^2 = k^2 + q^2 + 2kqy, \quad q'^2 = k^2 + p^2 + 2kpz, \qquad (2.12)\text{–}(2.14)$$

we get the following inequality:

$$dD/dt \geqslant tD^2/3(1 + 3\lambda t D^{\frac{1}{2}}), \qquad (2.15)$$

which shows that enstrophy blows up at a finite time $t_* \leqslant (9\lambda + 6^{\frac{1}{2}})D^{-\frac{1}{2}}(0)$ (see appendix A). Such a change in $\theta_{kpq}(t)$ can be justified while one is interested in local interactions.

(*c*) The numerical integration of (2.2) for very large Reynolds numbers does, however, show that the rate of energy dissipation increases dramatically after a finite time t_* of order $5k_I^{-1}\langle \mathbf{u}^2(0) \rangle^{-\frac{1}{2}}$ (figure 4), and it is reasonable to infer that, in the formal limit of infinite Reynolds number, energy dissipation will still begin at time t_*, owing to a blow-up of the enstrophy.

Figure 5 shows the time evolution of the skewness factor for various values of the Reynolds number: it can be seen that for a given t ($> t_*$) the skewness factor increases with Reynolds number and tends to the value 0·495. This value is in good agreement with the low Reynolds number value of 0·47 obtained in the direct numerical simulation of Orszag & Patterson (1972). On the other hand, we made low Reynolds number calculations using the EDQN theory under the same conditions as in the above-quoted numerical simulations and found a skewness factor of 0·39. This discrepancy between the EDQN theory and the direct calculations may be ascribed to the adjustment of the parameter λ to the Kolmogorov constant, which is justified only when there is a Kolmogorov energy cascade, i.e. at high Reynolds numbers. It would perhaps be

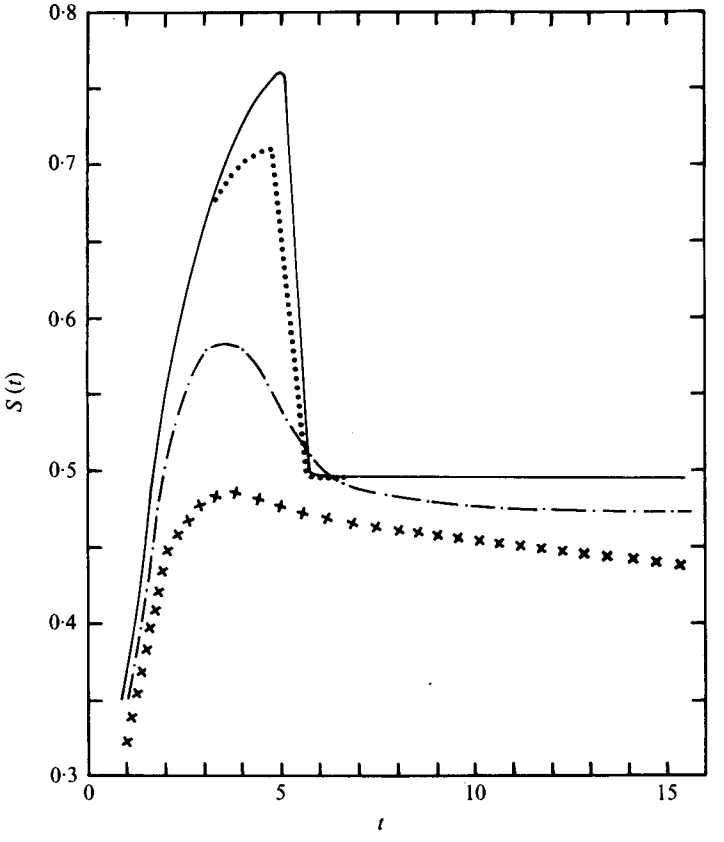

FIGURE 5. Temporal evolution of the skewness factor; same initial conditions as in figure 1. Curves as in figure 4.

necessary to adjust λ in terms of the skewness factor in order to use the EDQN theory at low Reynolds numbers. (The value 0·39 is, however, in good agreement with experimental results reported by Batchelor 1953, p. 118.)

3. Temporal evolution of helical turbulence

When helicity is present the EDQN equations for the energy spectrum $E(k,t)$ and the helicity spectrum $H(k,t)$ are (Lesieur 1973)

$$\left(\frac{\partial}{\partial t}+2\nu k^2\right)E(k,t)=\frac{1}{2}\iint_{\Delta_k}\frac{k}{pq}\theta_{kpq}(t)\,b_3(k,p,q)\{k^2E(p,t)\,E(q,t)-p^2E(q,t)\,E(k,t)\}\,dp\,dq$$
$$-\frac{1}{2}\iint_{\Delta_k}\frac{k}{p^3q}\theta_{kpq}(t)\,c(k,p,q)\{k^2H(p,t)\,H(q,t)-p^2H(q,t)\,H(k,t)\}\,dp\,dq, \quad (3.1)$$

$$\left(\frac{\partial}{\partial t}+2\nu k^2\right)H(k,t)=\frac{1}{2}\iint_{\Delta_k}\frac{k}{pq}\theta_{kpq}(t)\,b_3(k,p,q)\{k^2H(p,t)\,E(q,t)-p^2E(q,t)\,H(k,t)\}\,dp\,dq$$
$$-\frac{1}{2}\iint_{\Delta_k}\frac{k^3}{pq}\theta_{kpq}(t)\,c(k,p,q)\{E(p,t)\,H(q,t)-H(q,t)\,E(k,t)\}\,dp\,dq, \quad (3.2)\dagger$$

† Equations similar to (3.1) and (3.2) can also be given for other theories; in appendix B the reader will find such a set of equations generalizing Kraichnan's DIA equations to the helical case.

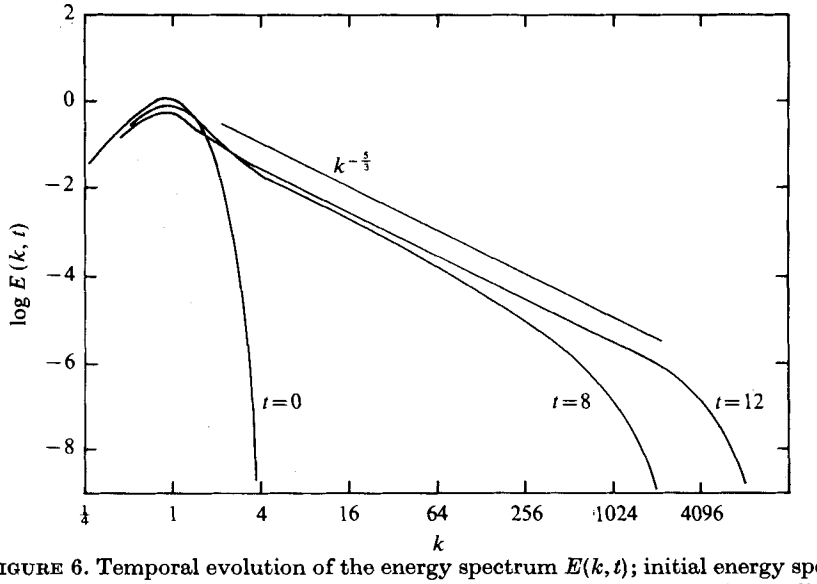

FIGURE 6. Temporal evolution of the energy spectrum $E(k,t)$; initial energy spectrum $E(k,0) \sim k^4 \exp(-2k^2)$, Reynolds number $R = 524000$, maximal initial helicity.

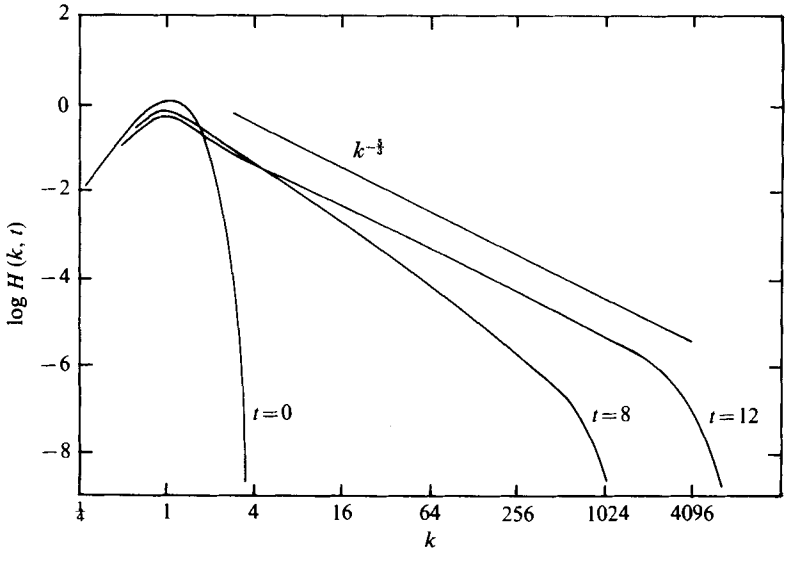

FIGURE 7. Temporal evolution of the helicity spectrum $H(k,t)$; same conditions as in figure 6.

where $\theta_{kpq}(t)$ is defined by (1.4) and

$$b_3(k,p,q) = (p/k)\,(xy+z^3), \quad c(k,p,q) = (p^2/kq)\,z(x+yz). \tag{3.3}$$

We have integrated (3.1) and (3.2) numerically starting with maximal initial helicity,

$$H(k,0) = kE(k,0), \tag{3.4}$$

and $E(k,0)$ given by (2.8). The Reynolds number defined by (2.7) is equal to 524 000 as in the preceding section. We decided to use in the helical case the same expressions (1.4) and (1.5) for the triple-correlation relaxation time as in the non-helical case.

Figures 6 and 7 show the evolution of the energy and helicity spectra. It is seen that the appearance of an inertial range is delayed roughly by a factor 2. This is consistent with the investigation of Kraichnan (1973), who considered the interaction between two helicity waves (Moffatt 1970*a*, *b*; Lesieur *et al.* 1971; Mazure 1972) and showed that there was an inhibition of energy transfer, and also with low Reynolds number DIA calculations by Herring. Figures 6 and 7 clearly establish the existence of simultaneous energy and helicity cascades as conjectured by Brissaud *et al.* (1973*a*):

$$E(k) = C_E \epsilon^{\frac{2}{3}} k^{-\frac{5}{3}}, \tag{3.5}$$

$$H(k) = C_H \eta \epsilon^{-\frac{1}{3}} k^{-\frac{5}{3}}, \tag{3.6}$$

where η is the helicity dissipation rate; C_E and C_H are respectively the Kolmogorov constants of the energy and helicity inertial ranges. It can be seen in figures 8(*a*) and (*b*) that the compensated spectra $k^{\frac{5}{3}}E(k)\epsilon^{-\frac{2}{3}}$ and $k^{\frac{5}{3}}H(k)\epsilon^{\frac{1}{3}}\eta^{-1}$ remain respectively equal (to within 10 %) to 1·76 and 2·84 from $k = 4$ to $k = 512$. The value 2·84 for C_H will be determined precisely in § 4. It must be noticed that the helicity spectrum obeys the same law as the spectrum of a passive scalar carried along by turbulence: since a passive scalar obeys a linear equation, its spectrum $\phi(k)$ is proportional to its injection rate σ; the usual Kolmogorov arguments applied to $\phi(k)/\sigma$ then give $\phi(k) \sim \sigma\epsilon^{-\frac{1}{3}}k^{-\frac{5}{3}}$ (Oboukhov 1949; Corrsin 1951; Batchelor 1959). We may therefore say that helicity cascades linearly. In fact, the same phenomenological arguments as those used by Brissaud *et al.* (1973*a*) show that, if one takes the same relaxation rate μ_k for triple correlations, one obtains a linear cascade for the helicity spectrum: $H(k) \sim \eta/\epsilon E(k)$. When μ_k depends on the helicity spectrum, one might expect the Kolmogorov law to be modified by helicity. But since in the linear cascade the relative helicity $H(k)/kE(k)$ goes to zero when k goes to infinity, helicity has a negligible effect for large wavenumbers and cannot modify the $k^{-\frac{5}{3}}$ energy spectrum. The situation may be rather different if one does not take the same value of μ_k in (3.1) and (3.2). In that case it is not certain that helicity should cascade linearly. The matter might be clarified through study of helical turbulence with the test-field model (Kraichnan 1971*a*; Sulem *et al.* 1975).

Figure 9 shows the relative helicity $H(k)/kE(k)$. As expected from (3.5) and (3.6), it goes to zero for large k. It will be shown in § 4 that the existence of simultaneous energy and helicity cascades requires $H(k)/kE(k) \lesssim 0{\cdot}1$. Figure 10 shows the rate of transfer of energy

$$\pi(K,t) = \int_K^\infty T_E(k,t)\,dk \tag{3.7}$$

and the rate of transfer of helicity

$$\Sigma(K,t) = \int_K^\infty T_H(k,t)\,dk, \tag{3.8}$$

where T_E and T_H respectively represent the right-hand sides of (3.1) and (3.2). For $t = 12$, $\pi(k)$ and $\Sigma(k)$ are constant to within 6 % and 5 % respectively from $k = 4$ to $k = 512$. Notice also that the rate of energy transfer into the inertial range has decreased by a factor of 2 compared with the non-helical case, which is expected since we know that the energy transfer is inhibited by helicity.

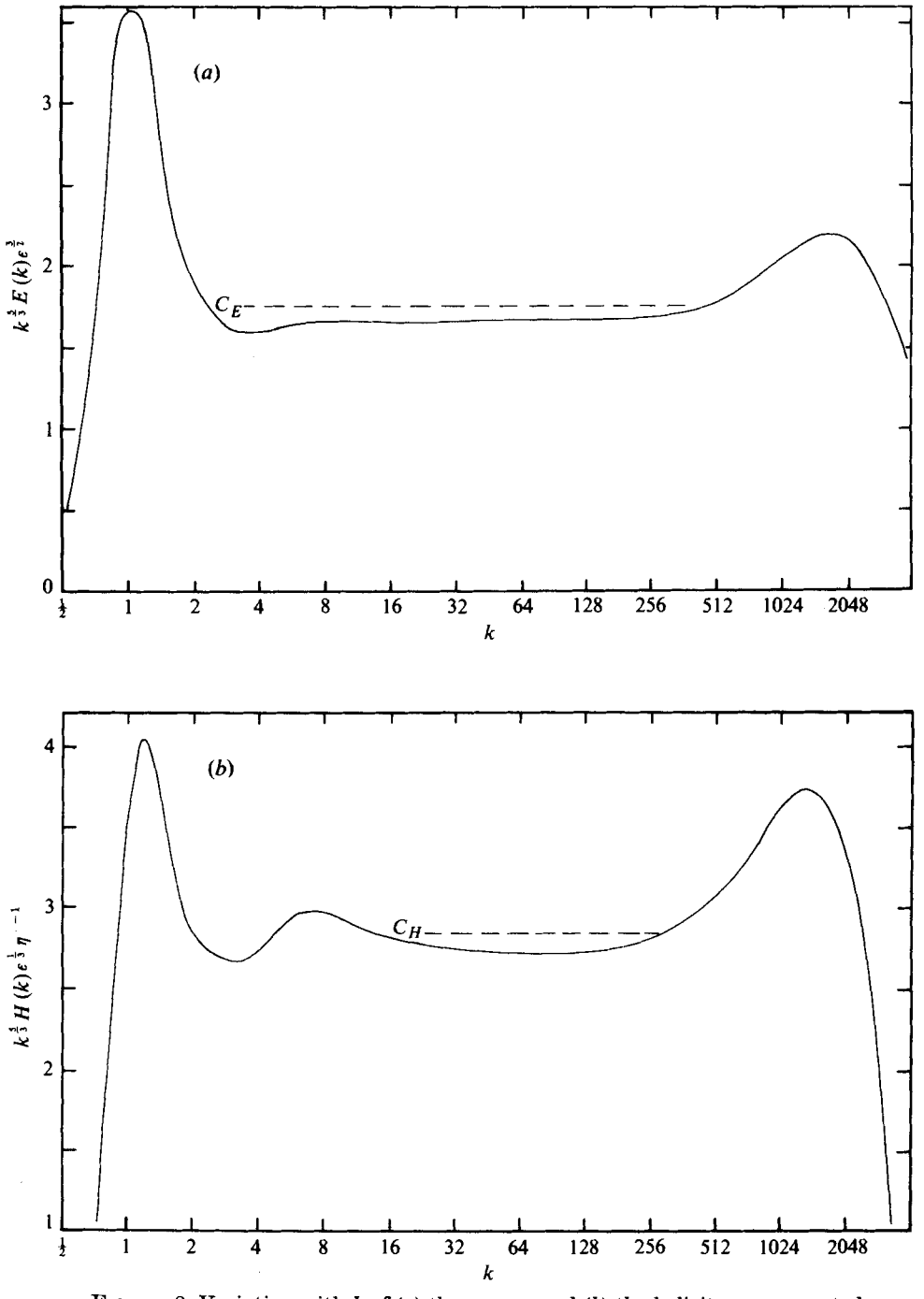

FIGURE 8. Variation with k of (*a*) the energy and (*b*) the helicity compensated spectra as defined in § 3 for $t = 12$; same conditions as in figure 6.

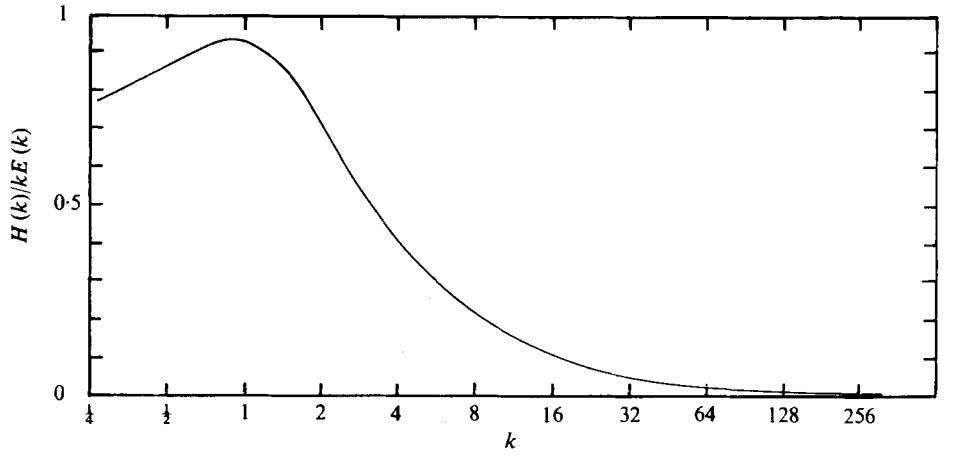

FIGURE 9. Variation with k of the relative helicity $H(k)/kE(k)$ for $t = 12$; same conditions as in figure 6.

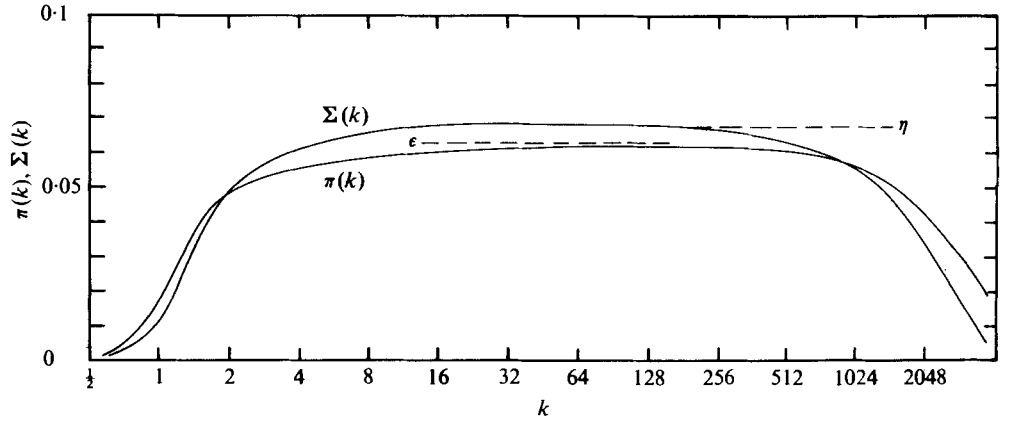

FIGURE 10. Variation with k of the energy and helicity transfer rates $\pi(k,t)$ and $\Sigma(k,t)$ for $t = 12$; same conditions as in figure 6. – – –, energy and helicity dissipation rates ϵ and η.

As a consequence of the inhibition of energy transfer by helicity we also expect the energy catastrophe to be delayed. An analytical study of this phenomenon based on (3.1) and (3.2) seems rather complicated. Numerically, the situation is much clearer. Figure 11 shows the temporal evolution of energy $\langle \mathbf{u}^2(t) \rangle$ and helicity $\langle \mathbf{u}(t) . \operatorname{curl} \mathbf{u}(t) \rangle$ for the above numerical calculation. We have checked that these curves are in fact the zero-viscosity limits in the same way as in figure 4 for the non-helical case. The catastrophe time t_*, which was $C_1/\langle \mathbf{u}^2(0) \rangle^{\frac{1}{2}} k_I$ (with $C_1 \approx 5$) without helicity, is now $C_2/\langle \mathbf{u}^2(0) \rangle^{\frac{1}{2}} k_I$ (with $C_2 \approx 9$) when the initial helicity is maximal. We must also notice that corresponding to the energy catastrophe there is a helicity catastrophe (onset of helicity dissipation at zero viscosity), which occurs at the same time as the energy catastrophe.

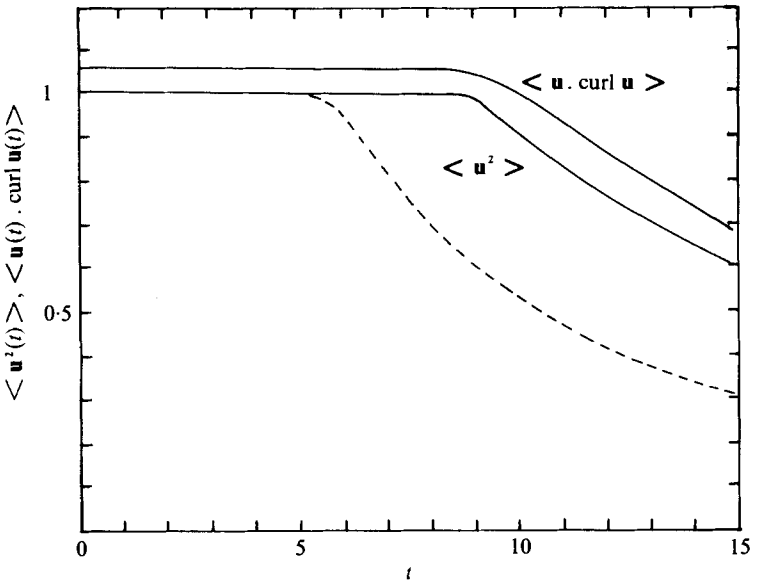

FIGURE 11. Temporal evolution of the total energy $\langle \mathbf{u}^2(t) \rangle$ and helicity $\langle \mathbf{u}(t) . \operatorname{curl} \mathbf{u}(t) \rangle$; same conditions as in figure 6. For comparison the dashed line represents the variation of total energy with no helicity reported in figure 4.

4. Determination of C_E and C_H: impossibility of a pure helicity cascade

Assuming energy and helicity spectra given by (3.5) and (3.6), it is possible to calculate the Kolmogorov constants C_E and C_H as functions of the parameter λ. For this, we use (3.5) and (3.6) to calculate T_E and T_H.† Following Kraichnan (1971*b*), we obtain

$$\pi(k) = \epsilon \int_0^1 Q_E(v) \frac{dv}{v} - \frac{\eta^2}{\epsilon k^2} \int_0^1 \widetilde{Q}_E(v) \frac{dv}{v}, \tag{4.1}$$

$$\Sigma(k) = \eta \int_0^1 Q_H(v) \frac{dv}{v}, \tag{4.2}$$

where $$Q_E(v) = \frac{C_E^{\frac{3}{2}}}{8(3)^{\frac{1}{2}}\lambda} A(v), \quad \widetilde{Q}_E(v) = \frac{C_H^2}{16(3)^{\frac{1}{2}}\lambda C_E^{\frac{1}{2}}} B(v), \quad Q_H(v) = \frac{C_H C_E^{\frac{1}{2}}}{8(3)^{\frac{1}{2}}\lambda} C(v), \tag{4.3)–(4.5}$$

in which the dimensionless functions $A(v)$, $B(v)$ and $C(v)$ are given in appendix C. The functions $Q_E(v) - (\eta^2/\epsilon^2 k^2)\, \widetilde{Q}_E(v)$ and $Q_H(v)$ give the contributions to the total energy and helicity transfer across the wavenumber k of triads with lower and middle wavenumbers in the ratio v. $Q_E(v)$ is the function $Q(v)$ of Kraichnan (1971*b*). From (4.1) we see that a true energy cascade ($\pi(k)$ independent of k) requires k sufficiently large so that

$$\frac{\eta^2}{\epsilon^2 k^2} \int_0^1 \widetilde{Q}_E(v) \frac{dv}{v} \ll \int_0^1 Q_E(v) \frac{dv}{v}. \tag{4.6}$$

† One might object that (3.5) and (3.6) are no longer valid for $k < C_E \eta / C_H \epsilon$, since the inequality (1.3) is violated. But these small k values give a negligible contribution to Q_E, $\widetilde{Q}_E$ and Q_H.

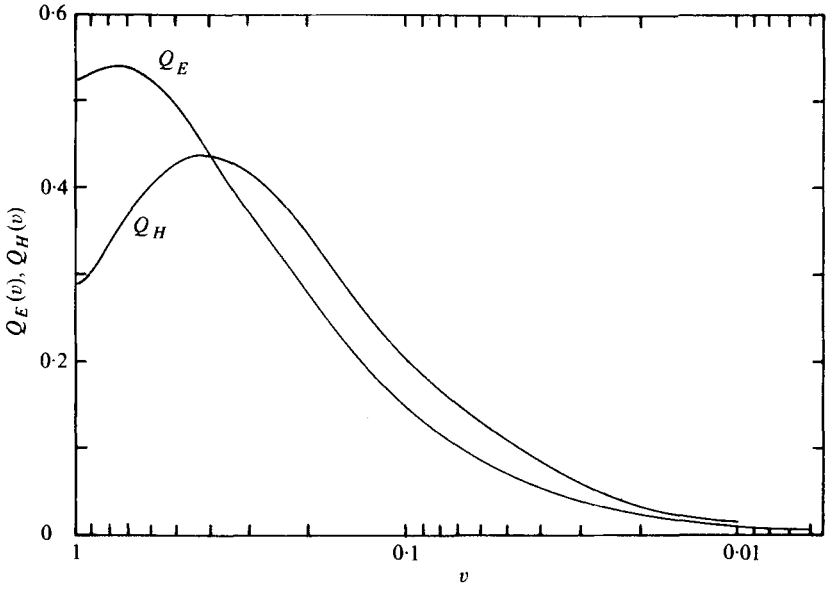

FIGURE 12. Localness of transfer of energy ($Q_E(v)$) and helicity ($Q_H(v)$).

When (4.6) is satisfied, (4.1) and (4.3) imply

$$\frac{C_E^{\frac{3}{2}}}{8(3)^{\frac{1}{2}}\lambda} = \left\{\int_0^1 A(v)\frac{dv}{v}\right\}^{-1}, \tag{4.7}$$

$$\frac{C_H C_E^{\frac{1}{2}}}{8(3)^{\frac{1}{2}}\lambda} = \left\{\int_0^1 C(v)\frac{dv}{v}\right\}^{-1}, \tag{4.8}$$

and finally a numerical calculation of the integrals

$$\int_0^1 A(v)\,v^{-1}\,dv, \quad \int_0^1 C(v)\,v^{-1}\,dv$$

yields $$C_E = 4{\cdot}38\lambda^{\frac{2}{3}}, \quad C_H = 7{\cdot}07\lambda^{\frac{2}{3}}. \tag{4.9), (4.10}$$

For $\lambda = 0{\cdot}255$, C_E and C_H are respectively equal to 1·76 and 2·84. Note that (4.9) is also valid in the non-helical case, so that the Kolmogorov constant C_E is not modified by helicity. In the inertial range, the relative helicity is then equal to

$$H(k)/kE(k) = 1{\cdot}43k^{-1}(\eta/\epsilon). \tag{4.11}$$

Now $$\int_0^1 \widetilde{Q}_E(v)\,v^{-1}\,dv = 3{\cdot}38,$$

so that inequality (4.6) gives $k \gg k_{\min} = 1{\cdot}85\eta/\epsilon$. In practice, an energy transfer constant to within 1 % will be obtained as soon as $k > 18{\cdot}5\eta/\epsilon$, which gives a maximum value of 0·08 for the relative helicity in the inertial range. Figure 12 shows $Q_E(v)$ and $Q_H(v)$ with C_E and C_H given by (4.9) and (4.10). It can be seen that $Q_E(v)$ is a maximum for $v = 0{\cdot}73$, while $Q_H(v)$ is a maximum for $v = 0{\cdot}425$, so that the helicity transfer is less local than the energy transfer. This point can be seen more clearly

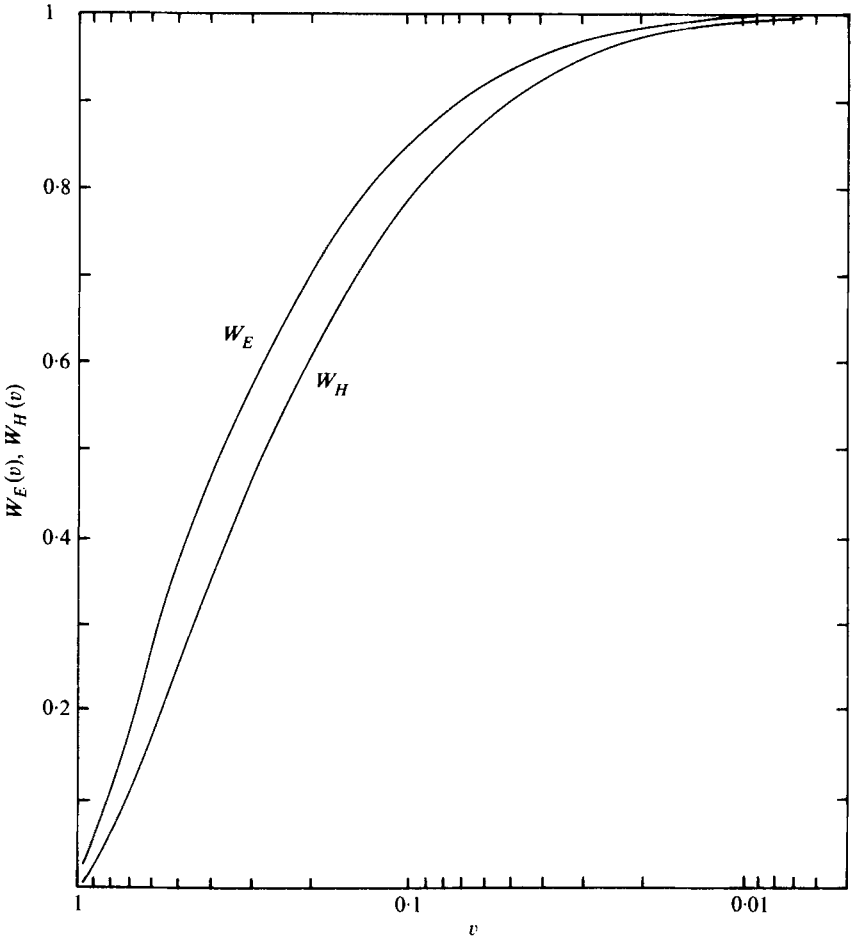

FIGURE 13. $W_E(v)$ and $W_H(v)$.

in figure 13, which shows the functions $W_E(v)$ and $W_H(v)$ introduced by Kraichnan (1971*b*):

$$W_E(v) = \int_v^1 Q_E(s)\frac{ds}{s}, \quad W_H(v) = \int_v^1 Q_H(s)\frac{ds}{s}, \qquad (4.12), (4.13)$$

which represent the fractions of the energy and helicity transfer rates due to triad interactions for which the ratio between the lower and the middle wavenumbers is greater than v. For instance, to obtain 50 % of the energy transfer it is necessary to consider triads such that $v \geqslant 0{\cdot}37$, while one must take triads such that $v \geqslant 0{\cdot}28$ to obtain 50 % of the helicity transfer.

It is possible now to show the non-existence of the type (ii) pure helicity cascade (see § 1) considered by Brissaud *et al.* (1973*b*), at any rate within the present framework of the EDQN theory. Assume an inverse energy cascade towards small wavenumbers with no helicity transfer: then the energy and helicity spectra will be functions of ϵ and k, and will take the form

$$E(k) = C'_E \epsilon^{\frac{2}{3}} k^{-\frac{5}{3}}, \quad H(k) = C'_H \epsilon^{\frac{2}{3}} k^{-\frac{2}{3}}, \qquad (4.14), (4.15)$$

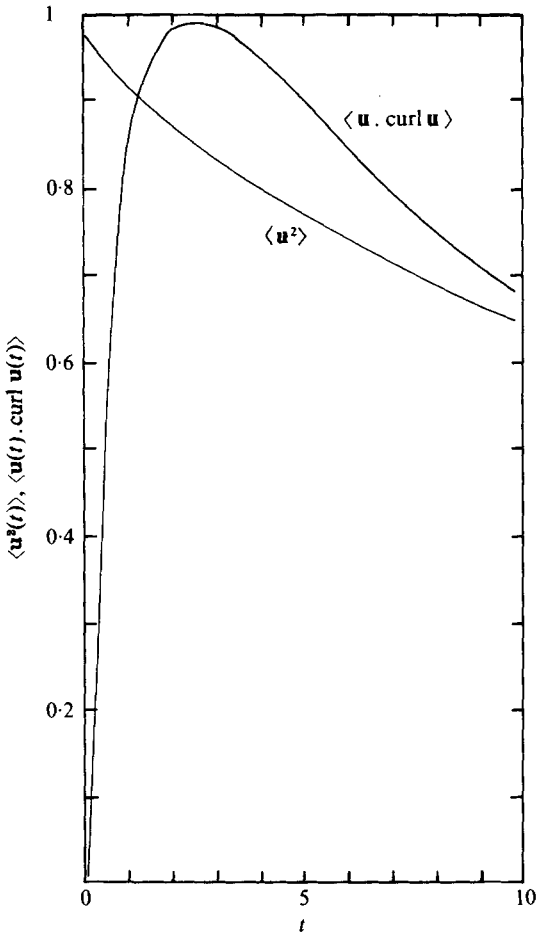

FIGURE 14. Temporal evolution of total energy $\langle \mathbf{u}^2(t) \rangle$ and helicity $\langle \mathbf{u}(t).\text{curl } \mathbf{u}(t) \rangle$ with zero initial total helicity; initial helicity and energy spectra defined in § 5.

C'_H being smaller than C'_E because of inequality (1.3). If we use (4.14) and (4.15) to calculate $T_E(k,t)$, we find for $\pi_E(k)$

$$\pi_E(k) = XC_E'^{\frac{3}{2}} - (C_H'^2/C_E'^{\frac{1}{2}})\, Y, \tag{4.16}$$

where X and Y are two integrals satisfying $Y < X$ (from numerical evaluation). Hence $\pi_E(k)$ is always positive, in contradiction with the hypothesis of an inverse energy cascade. The type (ii) cascade cannot therefore occur.

5. Possible growth of helicity through dissipation

Unlike the energy spectrum, the helicity spectrum $H(k)$ is not restricted to positive values. For example in the run corresponding to figure 7, the helicity spectrum takes negative values at the upper end of the dissipation range (i.e. for $k > 10^4 k_I$) in spite of purely positive initial values. These values naturally cannot be presented on figure 7 since a log–log plot is used (concerning figures 8*b* and 9, these negative values affect

wavenumbers which are not represented on the plots and anyway give very small values for the compensated spectrum and the relative helicity). Furthermore, the total helicity

$$H_T = \int_0^\infty H(k)\,dk$$

can grow and reach a significant level starting from a zero initial value. Indeed, if one starts from an initial helicity spectrum given by

$$H(k,0) = \pm kE(k,0) \quad \text{for} \quad k \leqslant k_c, \tag{5.1}$$

where k_c is a wavenumber chosen such that the total helicity is zero, then the helicity dissipation rate

$$\frac{d}{dt}\langle \mathbf{u}(t).\operatorname{curl}\mathbf{u}(t)\rangle_{t=0} = -2\nu\int_0^\infty k^2 H(k,0)\,dk \tag{5.2}$$

is certainly positive at $t = 0$. As a numerical illustration of this point, figure 14 shows the evolution of total energy and total helicity in the following case: we take for the initial energy spectrum $E(k,0)$ the energy spectrum obtained at $t = 6$ in the numerical calculation reported in § 2. In this case the value of k_c is found to be $8k_I$. One can see that the total helicity rapidly reaches a value of order unity, then decreases because of dissipation at a rate comparable to the energy dissipation rate.

6. Conclusion

The main influence of helicity in neutral isotropic turbulence seems to be the inhibition of energy transfer. However, this inhibition occurs in the early stages of decay, and disappears with the establishment of an inertial range. The basic spectral results, e.g. the Kolmogorov law, are not affected by helicity since the linear cascade of helicity implies a relative helicity which tends to zero for large wavenumbers.

In fact, though some recent results of Kraichnan (1976) seem to indicate that helicity increases the diffusion of a passive scalar by a factor of the order of 20 %, it seems likely that helicity is important only in the magnetohydrodynamic context. Indeed the study of absolute equilibrium ensembles shows the possibility of inverse transfer of energy in this context (Frisch *et al.* 1975), in contrast to the behaviour for neutral turbulence (Kraichnan 1973). Recent numerical results based on EDQN theory (Pouquet *et al.* 1976) and direct numerical simulation of the MHD equations (Pouquet & Patterson 1976) have confirmed the important influence of helicity in MHD turbulence.

We should like to thank J. R. Herring for having sent us his unpublished results. Thanks are also due to U. Frisch, J. Léorat, H. K. Moffatt and A. Pouquet for very helpful comments.

Appendix A. Proof of inequality (2.11)

From (2.2) one can easily derive the equation for the rate of change of the total enstrophy $D(t)$ in the inviscid case:

$$\frac{dD}{dt} = \frac{1}{2}\int\int\int \frac{k^2}{q}(k^2-p^2)(xy+z^3)\,\theta_{kpq}(t)\,E(p,t)\,E(q,t)\,dk\,dp\,dq. \tag{A 1}$$

By symmetrizing with respect to p and q and by making the change of variable $k \to x$ one finds

$$\frac{dD}{dt} = \frac{1}{4}\int_0^\infty\int_0^\infty p^2q^2E(p,t)\,E(q,t)\int_{-1}^{+1}\theta_{kpq}(t)\,(1-x^2)\,dx\,dp\,dq$$
$$-\frac{1}{4}\int_0^\infty\int_0^\infty pq(p^2+q^2)\,E(p,t)\,E(q,t)\int_{-1}^{+1}\theta_{kpq}(t)\,(1-x^2)\,x\,dx\,dp\,dq. \qquad (A\,2)$$

In the case of a constant relaxation time θ_0, the last integral on the right-hand side of (A 2) is zero since $\theta_0(1-x^2)\,x$ is odd, and (2.10) follows immediately.

This is no longer true for the EDQN theory, since the change $x \to -x$ changes θ_{kpq} into $\theta_{k'pq}$ with

$$k' = (p^2+q^2+2pqx)^{\frac{1}{2}}. \qquad (A\,3)$$

In this case, (A 2) becomes

$$\frac{dD}{dt} = \frac{1}{4}\int_0^\infty\int_0^\infty p^2q^2E(p,t)\,E(q,t)\int_{-1}^{+1}\theta_{kpq}(t)\,(1-x^2)\,dx\,dp\,dq$$
$$-\frac{1}{4}\int_0^\infty\int_0^\infty pq(p^2+q^2)\,E(p,t)\,E(q,t)\int_0^{+1}(\theta_{kpq}(t)-\theta_{k'pq}(t))\,(1-x^2)\,x\,dx\,dp\,dq. \qquad (A\,4)$$

With μ_k given by (1.5), μ_k increases with k and consequently $\theta_{kpq}(t)$ is a decreasing function of k. Notice that if, following Leith (1971), we had taken

$$\theta_{kpq}(t) = \frac{1-\exp\{-(\mu_k+\mu_p+\mu_q)\,t\}}{\mu_k+\mu_p+\mu_q} \qquad (A\,5)$$

instead of (1.4) [but keeping μ_k as given by (1.5)], $\theta_{kpq}(t)$ would still be a decreasing function of k. On the other hand this property is not necessarily satisfied either with Orszag's (1970) expression for μ_k,

$$\mu_k \sim (k^3E(k))^{\frac{1}{2}}, \qquad (A\,6)$$

or for the test-field model (Kraichnan 1971*a*).

The second integral on the right-hand side of (A 4) is then positive, so that we have

$$\frac{dD}{dt} \leqslant \frac{1}{4}\int_0^\infty\int_0^\infty p^2q^2E(p,t)\,E(q,t)\int_{-1}^{+1}\theta_{kpq}(t)\,(1-x^2)\,dx\,dp\,dq. \qquad (A\,7)$$

Since $\theta_{kpq}(t) \leqslant 1/(\mu_p+\mu_q)$, it follows that

$$\frac{dD}{dt} \leqslant \frac{1}{3}\int_0^\infty dp\int_0^\infty dq\,\frac{p^2q^2}{\mu_p+\mu_q}E(p,t)\,E(q,t) = \frac{2}{3}\int_0^\infty\int_0^p\frac{p^2q^2}{\mu_p+\mu_q}E(p,t)\,E(q,t)\,dp\,dq. \qquad (A\,8)$$

Taking the new variable μ_q, we have

$$\int_0^p\frac{q^2}{\mu_p+\mu_q}E(q,t)\,dq = \frac{2}{\lambda^2}\int_0^{\mu_p}\frac{\mu_q}{\mu_p+\mu_q}d\mu_q = 2(1-\log 2)\frac{\mu_p}{\lambda^2}, \qquad (A\,9)$$

and thus

$$\frac{dD}{dt} \leqslant \frac{8}{3}\frac{(1-\log 2)}{\lambda^4}\int_0^{\lambda D^{\frac{1}{2}}(t)}\mu^2\,d\mu = \frac{8}{9\lambda}(1-\log 2)\,D^{\frac{3}{2}}(t). \qquad (A\,10)$$

Hence, finally, with $\lambda = 0{\cdot}255$, the inequality (2.11) follows.

If we take $\phi_{kpq}(t) \equiv \theta_{lmn}(t)$, where $l = \sup(k,k')$, $m = \sup(p,p')$ and $n = \sup(q,q')$, instead of $\theta_{kpq}(t)$, (A 4) reduces to

$$\frac{dD}{dt} = \frac{1}{4}\int_0^\infty\int_0^\infty p^2q^2E(p,t)\,E(q,t)\int_{-1}^{+1}\phi_{kpq}(t)\,(1-x^2)\,dp\,dq\,dx. \qquad (A\,11)$$

Since $\phi_{kpq}(t) > t/(1+3\lambda t D^{\frac{1}{2}})$, it follows immediately that

$$dD/dt \geqslant tD^2/3(1+3\lambda t D^{\frac{1}{2}}). \tag{A 12}$$

As soon as $t \geqslant 6^{\frac{1}{2}} D^{-\frac{1}{2}}(0)$, since $D(t)$ increases with time ($dD/dt \geqslant 0$), (A 12) becomes

$$dD/dt \geqslant \frac{D^{\frac{3}{2}}}{3(3\lambda + 6^{-\frac{1}{2}})}. \tag{A 13}$$

Appendix B

Kraichnan's direct-interaction-approximation equations can be generalized for the helical case. These equations read

$$\begin{aligned}
&\left(\frac{\partial}{\partial t}+\nu k^2\right) U(k,t,t') \\
&\quad = \pi \iint_{\Delta_k} dp\,dq \int d\tau \{ -p^2 q b(k,p,q)\, g(p,t,\tau)\, U(q,t,\tau)\, U(k,\tau,t') \\
&\qquad + k^2 p q^2 c(k,p,q)\, g(p,t,\tau)\, \tilde{U}(q,t,\tau)\, \tilde{U}(k,\tau,t') \\
&\qquad - k^2 p^3 c(k,p,q)\, \tilde{g}(p,t,\tau)\, U(q,t,\tau)\, \tilde{U}(k,\tau,t') \\
&\qquad + p^3 q^2 c(k,p,q)\, \tilde{g}(p,t,\tau)\, \tilde{U}(q,t,\tau)\, U(k,\tau,t') \} \\
&\qquad + \frac{\pi}{2} \iint_{\Delta_k} dp\,dq \int d\tau \{ +kpq\, a(k,p,q)\, g(k,t',\tau)\, U(p,t,\tau)\, U(q,t,\tau) \\
&\qquad - kp^2 q^2 d(k,p,q)\, g(k,t',\tau)\, \tilde{U}(p,t,\tau)\, \tilde{U}(q,t,\tau) \\
&\qquad + 2k^2 p q^2 e(k,p,q)\, \tilde{g}(k,t',\tau)\, U(p,t,\tau)\, \tilde{U}(q,t,\tau) \},
\end{aligned} \tag{B 1}$$

$$\begin{aligned}
&\left(\frac{\partial}{\partial t}+\nu k^2\right) \tilde{U}(k,t,t') \\
&\quad = \pi \iint_{\Delta_k} dp\,dq \int d\tau \{ -p^2 q b(k,p,q)\, g(p,t,\tau)\, U(q,t,\tau)\, \tilde{U}(k,\tau,t') \\
&\qquad + pq^2 c(k,p,q)\, g(p,t,\tau)\, \tilde{U}(q,t,\tau)\, U(k,\tau,t') \\
&\qquad - p^3 c(k,p,q)\, \tilde{g}(p,t,\tau)\, U(q,t,\tau)\, U(k,\tau,t') \\
&\qquad + p^3 q^2 c(k,p,q)\, g(p,t,\tau)\, U(q,t,\tau)\, U(k,\tau,t') \} \\
&\qquad + \frac{\pi}{2} \iint_{\Delta_k} dp\,dq \int d\tau \{ +kpq\, a(k,p,q)\, \tilde{g}(k,t',\tau)\, U(p,t,\tau)\, U(q,t,\tau) \\
&\qquad - kp^2 q^2 d(k,p,q)\, \tilde{g}(k,t',\tau)\, \tilde{U}(p,t,\tau)\, \tilde{U}(q,t,\tau) \\
&\qquad + 2pq^2 e(k,p,q)\, g(k,t',\tau)\, U(p,t,\tau)\, U(q,t,\tau) \},
\end{aligned} \tag{B 2}$$

with the same notation as in Lesieur, Frisch & Brissaud (1971).

Appendix C

The dimensionless functions $A(v)$, $B(v)$ and $C(v)$ defined in § 4 are given by

$$A(v) = v \int_1^{1+v} \frac{dw}{1+v^{\frac{2}{3}}+w^{\frac{2}{3}}} \sum_\alpha w^\alpha (v f_\alpha(v) \log w + g_\alpha(v) \log v), \tag{C 1}$$

where α can take the values 5, $\frac{10}{3}$, 3, $\frac{4}{3}$, 1, $-\frac{2}{3}$, -1, $-\frac{8}{3}$ and $-\frac{14}{3}$ with

$$f_5(v) = -(1+v^2)\,v^{-\frac{17}{3}}, \quad g_5(v) = (2v^2-1)\,v^{-\frac{14}{3}},$$

$$f_{\frac{10}{3}}(v) = 0, \quad g_{\frac{10}{3}}(v) = v^{-\frac{14}{3}} - v^{-1},$$

$$f_3(v) = (1+6v^2+v^4)\,v^{-\frac{17}{3}}, \quad g_3(v) = (3-3v^2-4v^4)\,v^{-\frac{14}{3}},$$

$$f_{\frac{4}{3}}(v) = (2-v^2)\,v^{-\frac{17}{3}} + (2v^2-1)\,v^{-2}, \quad g_{\frac{4}{3}}(v) = -3(1+v^2)\,v^{-\frac{14}{3}} + (4+v^2)\,v^{-1},$$

$$f_1(v) = (1+v^2)\,(1-v^2)^2\,v^{-\frac{17}{3}}, \quad g_1(v) = -(1-v^2)^2\,(3+2v^2)\,v^{-\frac{14}{3}},$$

$$f_{-\frac{2}{3}}(v) = -(4+3v^2-3v^4)\,v^{-\frac{17}{3}} + (3-3v^2-4v^4)\,v^{-2},$$

$$g_{-\frac{2}{3}}(v) = (3+4v^2+3v^4)\,v^{-\frac{14}{3}} - (6+v^2-v^4)\,v^{-1},$$

$$f_{-1}(v) = -(1-v^2)^4\,v^{-\frac{17}{3}}, \quad g_{-1}(v) = (1-v^2)^3\,v^{-\frac{14}{3}},$$

$$f_{-\frac{8}{3}}(v) = (1-v^2)\,[(2-v^2+3v^4)\,v^{-\frac{17}{3}} - (3-v^2+2v^4)\,v^{-2}],$$

$$g_{-\frac{8}{3}}(v) = -(1+v^2)^3\,v^{-\frac{14}{3}} + (4-v^2+6v^4-v^6)\,v^{-1},$$

$$f_{-\frac{14}{3}}(v) = -(1-v^2)^3\,(v^{-\frac{11}{3}} - v^{-2}), \quad g_{-\frac{14}{3}}(v) = (1-v^2)^2\,[2v^{-\frac{8}{3}} - (1+v^2)\,v^{-1}];$$

$$B(v) = \int_1^{1+v} \frac{dw}{1+v^{\frac{8}{3}}+w^{\frac{8}{3}}} \sum_\beta w^\beta h_\beta(v), \tag{C 2}$$

where β can take the values 7, 5, $\frac{10}{3}$, 3, $\frac{4}{3}$, 1, $-\frac{2}{3}$, -1, $-\frac{8}{3}$ and $-\frac{14}{3}$ with

$$h_7(v) = -2v^{-\frac{11}{3}}, \quad h_5(v) = 5(1+v^2)\,v^{-\frac{11}{3}}, \quad h_{\frac{10}{3}}(v) = 1+v^{-\frac{11}{3}},$$

$$h_3(v) = -(3+2v^2+3v^4)\,v^{-\frac{11}{3}}, \quad h_{\frac{4}{3}}(v) = -(1+4v^2)\,v^{-\frac{11}{3}} - (4+v^2),$$

$$h_1(v) = -(1-v^2)\,(1-3v^4)\,v^{-\frac{11}{3}}, \quad h_{-\frac{2}{3}}(v) = (-3+v^2+6v^4)\,v^{-\frac{11}{3}} + (6+v^2-3v^4),$$

$$h_{-1}(v) = (1-v^2)^4\,v^{-\frac{11}{3}}, \quad h_{-\frac{8}{3}}(v) = (1-v^2)\,[(5+3v^2+4v^4)\,v^{-\frac{11}{3}} - (4+3v^2+5v^4)],$$

$$h_{-\frac{14}{3}}(v) = (1-v^2)^3\,[-(2+v^2)\,v^{-\frac{11}{3}} + (1+2v^2)];$$

$$C(v) = v\int_1^{1+v} \frac{dw}{1+v^{\frac{8}{3}}+w^{\frac{8}{3}}} \sum_\gamma w^\gamma (d_\gamma(v)\log w + e_\gamma(v)\log v), \tag{C 3}$$

where γ can take the values 5, $\frac{10}{3}$, 3, $\frac{4}{3}$, 1, $-\frac{2}{3}$, -1, $-\frac{8}{3}$ and $-\frac{14}{3}$ with

$$d_5(v) = 0, \quad e_5(v) = -(1-v^2)\,v^{-\frac{14}{3}},$$

$$d_{\frac{10}{3}}(v) = -(v^{-\frac{14}{3}} + v^{-1}), \quad e_{\frac{10}{3}}(v) = v^{-\frac{14}{3}},$$

$$d_3(v) = 0, \quad e_3(v) = 3(1-v^2)\,(1+v^2)\,v^{-\frac{14}{3}},$$

$$d_{\frac{4}{3}}(v) = (3+2v^2)\,v^{-\frac{14}{3}} + (2+3v^2)\,v^{-1}, \quad e_{\frac{4}{3}}(v) = -(3+2v^2)\,v^{-\frac{14}{3}},$$

$$d_1(v) = 0, \quad e_1(v) = -(1-v^2)\,(3+2v^2+3v^4)\,v^{-\frac{14}{3}},$$

$$d_{-\frac{2}{3}}(v) = -[(3+v^2)\,v^{-\frac{14}{3}} + (1+3v^2)\,v], \quad e_{-\frac{2}{3}}(v) = (3+v^2)\,v^{-\frac{14}{3}},$$

$$d_{-1}(v) = 0, \quad e_{-1}(v) = (1-v^2)^3\,(1+v^2)\,v^{-\frac{14}{3}},$$

$$d_{-\frac{8}{3}}(v) = (1-v^2)\,[(1+v^2+2v^4)\,v^{-\frac{14}{3}} - (2+v^2+v^4)\,v^{-1}],$$

$$e_{-\frac{8}{3}}(v) = -(1-v^2)\,(1+v^2+2v^4)\,v^{-\frac{14}{3}},$$

$$d_{-\frac{14}{3}}(v) = -(1-v^2)^3\,(v^{-\frac{8}{3}} - v^{-1}), \quad e_{-\frac{14}{3}}(v) = (1-v^2)^3\,v^{-\frac{8}{3}}.$$

REFERENCES

BASDEVANT, C., LESIEUR, M. & SADOURNY, R. 1976 Subgridscale modelling of enstrophy transfer in two-dimensional turbulence. *Preprint Laboratoire de Météorologie Dynamique, Paris.*

BATCHELOR, G. K. 1953 *The Theory of Homogeneous Turbulence.* Cambridge University Press.

BATCHELOR, G. K. 1959 *J. Fluid Mech.* **5**, 113.

BETCHOV, R. 1961 *Phys. Fluids* **4**, 925.

BRISSAUD, A., FRISCH, U., LÉORAT, J., LESIEUR, M. & MAZURE, A. 1973*a* *Phys. Fluids* **16**, 1366.

BRISSAUD, A., FRISCH, U., LÉORAT, J., LESIEUR, M., MAZURE, A., POUQUET, A., SADOURNY, R. & SULEM, P. L. 1973*b* *Ann. Geophys.* **29**, 539.

CORRSIN, S. 1951 *J. Appl. Phys.* **22**, 469.

EBIN, D. & MARSDEN, J. 1970 *Ann. Math.* **92**, 102.

FRISCH, U., LESIEUR, M. & BRISSAUD, A. 1974 *J. Fluid Mech.* **65**, 145.

FRISCH, U., LESIEUR, M. & SULEM, P. L. 1976 *Phys. Rev. Lett.* **37**, 895.

FRISCH, U., POUQUET, A., LÉORAT, J. & MAZURE, A. 1975 *J. Fluid Mech.* **68**, 769.

KATO, T. 1972 *J. Funct. Anal.* **9**, 296.

KRAICHNAN, R. H. 1971*a* *J. Fluid Mech.* **47**, 513.

KRAICHNAN, R. H. 1971*b* *J. Fluid Mech.* **47**, 525.

KRAICHNAN, R. H. 1973 *J. Fluid Mech.* **59**, 745.

KRAICHNAN, R. H. 1976 *J. Fluid Mech.* **77**, 753.

LEE, T. D. 1952 *Quart. Appl. Math.* **10**, 69.

LEITH, C. E. 1971 *J. Atmos. Sci.* **28**, 145.

LESIEUR, M. 1973 Ph.D. thesis, University of Nice.

LESIEUR, M., FRISCH, U. & BRISSAUD, A. 1971 *Ann. Geophys.* **27**, 151.

LESIEUR, M. & SULEM, P. L. 1976 In *Turbulence and Navier–Stokes Equations.* Springer.

MAZURE, A. 1972 Thesis, Observatoire de Meudon.

MOFFATT, H. K. 1969 *J. Fluid Mech.* **35**, 117.

MOFFATT, H. K. 1970*a* *J. Fluid Mech.* **41**, 435.

MOFFATT, H. K. 1970*b* *J. Fluid Mech.* **44**, 705.

OBOUKHOV, A. M. 1949 *Izv. Akad. Nauk USSR, Geogr. Geophyz.* **13**, 58.

ORSZAG, S. A. 1970 *J. Fluid Mech.* **41**, 363.

ORSZAG, S. A. 1976 In *Proc.* 1973 *Les Houches Summer School Theor. Phys.* Gordon & Breach.

ORSZAG, S. A. & PATTERSON, G. S. 1972 In *Statistical Models and Turbulence*, p. 127. Springer.

PENEL, P. 1975 Ph.D. thesis, University of Paris-Sud.

POUQUET, A., FRISCH, U. & LÉORAT, J. 1976 *J. Fluid Mech.* **77**, 321.

POUQUET, A., LESIEUR, M., ANDRÉ, J. C. & BASDEVANT, C. 1975 *J. Fluid Mech.* **72**, 305.

POUQUET, A. & PATTERSON, G. S. 1976 Numerical simulation of helical magnetohydrodynamic turbulence. *Preprint N.C.A.R., Boulder.*

PROUDMAN, I. & REID, W. H. 1954 *Phil. Trans. Roy. Soc.* A**247**, 163.

STEENBECK, M., KRAUSE, F. & RÄDLER, Z. 1966 *Z. Naturforsch.* A**21**, 364.

SULEM, P. L., LESIEUR, M. & FRISCH, U. 1975 *Ann. Geophys.* **31**, 52.